

# Direct unconstrained optimization of excited states in density functional theory

Hanh D. M. Pham and Rustam Z. Khaliullin

*Department of Chemistry, McGill University, 801 Sherbrooke St West, Montreal, QC H3A 0B8, Canada*

Email: rustam.khaliullin@mcgill.ca

(Dated: January 22, 2025)

**Abstract.** Orbital-optimized density functional theory (DFT) has emerged as an alternative to time-dependent (TD) DFT capable of describing difficult excited states with significant electron density redistribution, such as charge-transfer, Rydberg, and double-electron excitations. Here, a simple method is developed to solve the main problem of the excited-state optimization – the variational collapse of the excited states onto the ground state. In this method, called variable-metric time-independent DFT (VM TIDFT), the electronic states are allowed to be nonorthogonal during the optimization but their orthogonality is gradually enforced with a continuous penalty function. With nonorthogonal electronic states, VM TIDFT can use molecular orbital coefficients as independent variables, which results in a closed-form analytical expression for the gradient and allows to employ any of the multiple unconstrained optimization algorithms that guarantees convergence of the excited-state optimization. Numerical tests on multiple molecular systems show that the variable-metric optimization of excited states performed with a preconditioned conjugate gradient algorithm is robust and produces accurate energies for well-behaved excitations and, unlike TDDFT, for more challenging charge-transfer and double-electron excitations.

## INTRODUCTION

Excited electronic states play a crucial role in photo-physics and photochemistry<sup>1–3</sup>. Theoretical and computational characterization of excited states is essential, not only from a fundamental science perspective but also for designing better photovoltaic, photocatalytic, and lighting materials. One of the most popular methods to describe excited states is time-dependent (TD) density functional theory (TDDFT), which is an extension of the ground-state Kohn-Sham (KS) density functional theory (DFT). TDDFT calculates excited state properties by analyzing the response of the ground-state density to time-dependent perturbations, such as an external electric field<sup>4</sup>. Although TDDFT is, in principle, exact<sup>5</sup>, it has multiple limitations that arise from its reliance on time-independent ground state XC functionals<sup>4</sup>. Consequently, TDDFT cannot describe double- and higher-electron excitations and struggles with excitations producing significant changes of the electron density distribution, such as long-range charge transfer states, Rydberg states, and core excitations<sup>6,7</sup>.

To address the limitations of TDDFT, a variety of orbital optimized (OO) DFT methods have been developed. In these methods, the ground-state DFT formalism is applied to optimize orbitals variationally not only for the ground state but also for the excited states. To contrast this approach to TDDFT, it has been referred to as time-independent DFT (TIDFT)<sup>8–11</sup>.  $\Delta$ SCF is another commonly used name for this approach<sup>12–17</sup> which emphasizes that the excitation energies are computed as the energy difference between self-consistent-field (SCF) calculations. The variational treatment of the excited states yields excellent results, comparable to those ob-

tained with TDDFT for well-behaved excited states and superior for charge-transfer (CT) and multi-electron excitations<sup>18–24</sup>. Another advantage of using the ground-state formalism for excited states is that numerous techniques developed over several decades for KS DFT can be applied to excited states. For example, the implicit solvation models employed in ground states calculations can be readily used for excited states<sup>25,26</sup>.

While the effort to establish a solid theoretical foundation for the excited-state OODFT methods is underway<sup>8–11,17</sup>, the most significant practical challenge in designing efficient OODFT methods is ensuring that the variational optimization converges to the correct excited state rather than collapsing back to the ground state<sup>24</sup>. There has been a number of methods proposed to avoid variational collapse of high-energy excited states to the states with lower energies<sup>27–44</sup>. These methods have been recently reviewed<sup>6,30,45,46</sup> and only a brief description of some of them is presented here.

In the maximum overlap method (MOM)<sup>28</sup> and initial maximum overlap method (IMOM)<sup>47,48</sup>, the electrons are first promoted from the fully optimized ground-state occupied MOs to virtual MOs to generate the initial guess for an excited state. The newly selected occupied MOs are then optimized in the SCF procedure, in each step of which the list of occupied orbitals is updated using a non-aufbau population principle. In IMOM, the occupied orbitals are updated to maximize their overlap with the initial guess, whereas, in MOM, the orbitals are updated to produce maximum overlap with the orbitals in the previous SCF step. By maximizing the overlap with high-lying orbitals, MOM and IMOM prevent variational collapse to the ground state, guiding the SCF process toward the nearest excited state solution. Although both methods work well for multiple systems, MOM can-

not always prevent variational collapse, as orbitals can drift to the ground state over multiple steps<sup>47–49</sup>. While this issue is addressed in IMOM, the latter exhibits its own convergence problems when multiple orbital selections have similar overlaps, which produces oscillatory non-convergent behavior<sup>38,39</sup>.

An alternative approach to prevent variational collapse is to constrain the KS determinant of an excited state to be orthogonal to that of the ground state. In practice, orthogonality-constrained DFT (OCDFT)<sup>32</sup> recasts the optimization problem as a solution to modified eigenvector equations and imposes this constraint by projecting out a single “hole” orbital from the KS Hamiltonian. Unfortunately, the iterative solution of eigenvector problems is not guaranteed to converge. Furthermore, the projector-based formalism of OCDFT makes its extension to multiple excited states cumbersome.

To improve the rate of convergence, several direct minimization algorithms have been developed. For example, the ground-state geometric direct minimization (GDM) approach<sup>50</sup> has been extended to optimize excited states with the IMOM orbital-selection criterion applied on each GDM iteration to prevent the collapse<sup>35,36,41,44</sup>. While the combination of GDM and IMOM resolves some of the convergence issues of the original eigensolver-based MOM, the combined method still does not guarantee convergence because the application of the IMOM criterion is introduced as an *ad hoc* update, which can interfere with the GDM optimizer.

Another direct optimization approach is square gradient minimization (SGM)<sup>39</sup>. SGM minimizes the square of the Frobenius norm of the energy gradient instead of minimizing the energy and thereby converts the saddle-point excited-state optimization into the minimization problem, obviating the need in any collapse prevention measures. Despite being superior to MOM-based methods in terms of convergence for difficult problems, SGM has its own shortcomings, as the norm of the gradient is less well conditioned than the energy, typically requiring more iterations to converge for simple cases<sup>39,51</sup>. Furthermore, SGM can become trapped in local minima that are not stationary points of the energy functional<sup>39</sup>.

This work presents a new approach to the variational optimization of excited electronic states, called variable-metric (VM) TIDFT. Like OCDFT, VM TIDFT prevents the variational collapse by imposing orthogonality constraints between electronic states. Unlike OCDFT, VM TIDFT allows nonorthogonal electronic states in the optimization process but pushes them towards orthogonality with a single continuous penalty function. The key advantage of VM TIDFT is the simplicity of its formalism that allows to relax multiple excited states using molecular orbital coefficients as independent variables in a direct unconstrained minimization that guarantees convergence of the SCF procedure. VM optimization has been designed specifically to prevent collapse of non-orthogonal

wavefunctions and has been previously applied to improve localization of occupied and virtual orbitals<sup>52,53</sup> and to simplify the ground-state SCF procedure<sup>54</sup>.

## METHODOLOGY

**Theory.** In our notation, capital Latin letters ( $I, J, K, \dots$ ) denote electronic states, lowercase Latin letters ( $i, j, k, \dots$ ) denote occupied molecular orbitals, and lowercase Greek letters ( $\mu, \nu, \gamma, \lambda, \dots$ ) represent basis set functions. Additionally, Greek letters  $\alpha$  and  $\beta$  are reserved for spin-up and spin-down electrons, respectively, whereas the symbol  $\tau$  denotes a general spin state.

The unrestricted VM TIDFT formalism presented here optimizes  $\alpha$  and  $\beta$  orbitals independently to take into account the open-shell nature of excited states. However, restricted closed-shell (RKS), restricted-open shell (ROSO), and spin-purified restricted open-shell Kohn-Sham (ROKS)<sup>55,56</sup> optimization of excited states can also be performed as described previously for the ground state<sup>54</sup>.

The optimization of multiple excited states is performed state-by-state. The loss functional minimized in the VM TIDFT procedure for electronic state  $I$  is a sum of the *intrastate* term  $\mathcal{E}^I$  and the *interstate* penalty term  $\Omega_P$

$$\Omega = \mathcal{E}^I + \Omega_P \quad (1)$$

The intrastate term includes  $E^I$  the energy of state  $I$  and the intrastate penalty that ensures linear independence of MOs of state  $I$

$$\mathcal{E}^I = E^I - c_P^I \sum_{\tau=\alpha,\beta} \ln \det(\sigma_{II\tau} \sigma_{II\tau d}^{-1}) \quad (2)$$

where  $\sigma_{II\tau}$  is the overlap matrix for the occupied orbitals of spin  $\tau$ , and  $\sigma_{II\tau d}$  is its diagonal part. The intrastate term was described in our previous treatment of the simple ground-state orbital optimization method<sup>54</sup>.

The interstate term is designed to keep different electronic states orthogonal to each other

$$\Omega_P = -C_P \sum_{\tau=\alpha,\beta} \ln \det(\Phi_\tau \Phi_{\tau d}^{-1}) \quad (3)$$

In the state-by-state optimization, the orthogonality penalty is imposed between the currently optimized state and all previously optimized states. The key element of the penalty is  $\Phi_\tau$  – the overlap matrix between electronic states.  $\Phi_{\tau d}$  is a diagonal matrix containing the elements of  $\Phi_\tau$ . Element  $(\Phi_\tau)_{IJ}$  of the state overlap matrix can be calculated as the determinant of the overlap of MOs that describe states  $I$  and  $J$

$$(\Phi_\tau)_{IJ} = \det(\sigma_{IJ\tau}) \quad (4)$$

where the MO overlap matrix of occupied orbitals

$$(\sigma_{IJ\tau})_{ij} = \sum_{\mu\nu}^B T_{\mu i}^{I\tau} S_{\mu\nu} T_{\nu j}^{J\tau} \quad (5)$$

is written using coefficients  $T_{\mu i}^{I\tau}$  that represent occupied MOs  $\phi_i^{I\tau}(\mathbf{r})$  in terms of  $B$  basis set functions  $\chi_\mu(\mathbf{r})$

$$\phi_i^{I\tau}(\mathbf{r}) = \sum_{\mu}^B \chi_\mu(\mathbf{r}) T_{\mu i}^{I\tau} \quad (6)$$

Here,  $S_{\mu\nu}$  is the overlap between basis set functions  $\mu$  and  $\nu$

$$S_{\mu\nu} = \int \chi_\mu(\mathbf{r}) \chi_\nu(\mathbf{r}) d\mathbf{r} \quad (7)$$

For non-zero orbitals, the positive determinant in the penalty term in Eq. (3) is equal to zero when there is linear dependency between electronic states.  $\Phi_{\tau d}$  is the normalization factor that ensures the determinant in the penalty functional does not exceed 1. The determinant achieves its highest value of 1 only when all electronic states are orthogonal. With  $\det(\Phi_\tau \Phi_{\tau d}^{-1})$  always kept in the  $(0, 1]$  interval, the logarithm function  $\Omega_P$  lies in the  $(+\infty, 0]$  interval, making the linearly dependent states and states with orbitals of zero norm inaccessible in the variational procedure, for any  $C_P > 0$ . A similar penalty term has proven effective to prevent orbital collapse during the SCF optimization of ground-state MOs<sup>54</sup> and during the localization of nonorthogonal occupied and virtual orbitals<sup>52,53</sup>.

The key benefit of introducing the interstate penalty term is that it allows to use molecular orbital coefficients – arguably the most natural descriptors of the electronic degrees of freedom – as independent variables in the optimization procedure. As shown below, the expressions for the analytical gradient of the loss functional wrt these variables are very simple and can be written in a closed form, making it easy to use a multitude of well-developed unconstrained optimization algorithms, including conjugate gradient algorithms, quasi-Newton algorithms, or trust-region algorithms<sup>57</sup>.

The gradient of the intrastate term with respect to orbital coefficients is described in our previous work:

$$\begin{aligned} G_{\mu i}^{I\tau\mathcal{E}} &\equiv \frac{\partial \mathcal{E}^I}{\partial T_{\mu i}^{I\tau}} \\ &= 2[(I - SP^{I\tau})F^{I\tau}T^{I\tau}(\sigma_{II\tau}^{-1})]_{\mu i} - \\ &\quad - 2c_p^I [ST^{I\tau}(\sigma_{II\tau}^{-1} - \sigma_{II\tau d}^{-1})]_{\mu i} \end{aligned} \quad (8)$$

where  $F^{I\tau}$  and  $P^{I\tau}$  are the Kohn-Sham Hamiltonian and density matrices, respectively, for state  $I$  and spin  $\tau$ . The density matrix is evaluated taking into account

nonorthogonality of occupied orbitals:

$$P_{\mu\nu}^{I\tau} = \sum_{ij}^{N_\tau} T_{\mu i}^{I\tau} (\sigma_{II\tau}^{-1})_{ij} T_{\nu j}^{I\tau} \quad (9)$$

The first derivatives of the interstate penalty term  $\Omega_P$  can also be evaluated analytically and computed readily

$$\begin{aligned} G_{\mu i}^{I\tau P} &\equiv \frac{\partial \Omega_P}{\partial T_{\mu i}^{I\tau}} = \\ &\quad - 2C_P \left[ \sum_J (\Phi_\tau)_{IJ}^{-1} [ST^{J\tau} \text{adj}(\sigma_{IJ\tau})]_{\mu i} - (ST^{I\tau} \sigma_{II\tau}^{-1})_{\mu i} \right] \end{aligned} \quad (10)$$

where  $\text{adj}(\sigma_{IJ\tau})$  is the adjugate of the singular or nearly-singular (i.e. ill-conditioned) overlap matrix between orbitals of states  $I$  and  $J$ . This adjugate matrix emerges from differentiating the determinant of the overlap matrix (see Supporting Information).

**Optimization algorithm.** In this work, VM TIDFT methods is implemented using the basic preconditioned conjugate gradient (PCG) algorithm for nonlinear problems<sup>58</sup>. To minimize a function, PCG needs only its first derivative (i.e. gradient). Computation of the exact second derivative is not required, but approximate second derivative has been found useful for the construction of accurate preconditioners, which increase the rate of convergence of the PCG algorithm and making it practical.

The analytical gradient of the intrastate term in Eq. (8) can be computed efficiently as done in our previous work. However, the analytical gradient of the interstate term requires the evaluation of the lesser known adjugate matrix of  $\sigma_{IJ\tau}$  – the overlap between MOs of two electronic states. Fortunately, the adjugate of a matrix is well-conditioned even if the matrix itself is ill-conditioned<sup>59</sup>. This property is very important in our case because nearly orthogonal electronic states, which are often encountered during the optimization, produce ill-conditioned  $\sigma_{IJ\tau}$ .

Our algorithm for computing the adjugate is designed to avoid ill-conditioned intermediates<sup>59</sup>. It relies on computing the singular value decomposition of the overlap

$$\begin{aligned} \text{adj}(\sigma) &= \text{adj}(UdV^\dagger) = \text{adj}(V^\dagger)\text{adj}(d)\text{adj}(U) = \\ &= \det(V) \det(U) V \text{adj}(d) U^\dagger \end{aligned} \quad (11)$$

and then evaluating the adjugate of the diagonal matrix  $d$  using the relation between the co-factor of a matrix and its adjugate

$$[\text{adj}(d)]_{ii} = [C^\dagger]_{ii} = \left[ \prod_{j \neq i} d_{jj} \right]_{ii} \quad (12)$$

where  $C$  is the diagonal cofactor matrix of  $d$ . Note that the inversion of singular values is not required in this

algorithm, making the algorithm stable for the often encountered ill conditioned matrices.

The preconditioner is constructed by simplifying the second derivative of the loss functional: the interstate term is neglected and the remaining intrastate term is approximated as described in the VM SCF optimization of a single electronic state<sup>54</sup>.

$$H_{\mu\nu}^{I\tau} = 4 \left[ (1 - \kappa) (A^{I\tau\dagger} F^{I\tau} A^{I\tau})_{\mu\nu} + \kappa |\varepsilon_{\text{HOMO}}| (D^{I\tau\dagger} S D^{I\tau})_{\mu\nu} \right] \quad (13)$$

where  $\kappa$  is a dimensionless regularization parameter that allows a user to increase the weight of the overlap in case of poor convergence<sup>54</sup>. Matrices  $A^{I\tau}$  and  $D^{I\tau}$  can be set to the projector onto the unoccupied subspace  $Q^{I\tau} \equiv (I - P^{I\tau} S)$ , identity matrix  $I$  or zero. This preconditioner is the same for all MOs of an electronic state and can be inverted independently for each state. The numerical tests described in the next section show that this preconditioner allows to optimize excited state MOs efficiently.

The computational cost of the PCG algorithm presented here is determined by both the number of the electronic states  $S$  and by the size of the system, that is, by the number electrons  $N$ , which is proportional to the number of basis set functions  $B$ . The cost of treating all  $S$  intrastate terms is dominated by the cost of inverting  $S$  preconditioners, which has  $\mathcal{O}(SB^3)$  computational complexity<sup>54,60</sup>. It should be noted that the preconditioners are inverted only in the beginning of the PCG procedure, making the direct optimization more efficient compared to the diagonalization-based methods, in which such costly operations are required on each iteration. It should also be noted that the intrastate cost of handling nonorthogonal MOs is lower –  $\mathcal{O}(SB^2N)$  to compute orbital overlaps  $\sigma_{II}$  and  $\mathcal{O}(SN^3)$  to invert them – because the number of electrons  $N$  is typically an order of magnitude lower than  $B$ . The determinants of the intrastate overlap matrices can also be computed relatively fast via their LU decomposition at  $\mathcal{O}(SN^3)$  cost.

Handling the interstate term and its derivative requires  $\mathcal{O}(S^2B^2N)$  time to build the  $S(S-1)/2$  overlap matrices for all pairs of electronic states,  $\mathcal{O}(S^2N^3)$  time to evaluate their adjugates and determinants (the latter being the elements of matrix  $\Phi$ ), and  $\mathcal{O}(S^3)$  time to compute the determinant of  $\Phi$ . Since the number of electronic states of interest is small compared to  $B^2N \gg S$  for most systems, building the overlap matrices will dominate the interstate computations.

To summarize, the intrastate and interstate terms are dominated by the  $\mathcal{O}(SB^3)$  and  $\mathcal{O}(S^2B^2N)$ , respectively. Therefore, the interstate term will represent the computational bottleneck for a large number of excited state, but does not consume significant computational time for most practical problems with  $S < 100$ .

Initial excited state orbitals are generated using fully optimized canonical ground-state orbitals. The guess is obtained by systematically generating all possible excitations involving a fixed number electrons, typically two, and then retaining only the lowest (unoptimized) energy excitations for further optimization.

**Penalty strength adjustment.** The interstate penalty term plays a critical role in preventing the collapse of high-energy states onto lower-energy states. Increasing the strength of this term by increasing  $C_P$  pushes the electronic states to become closer to being orthogonal. If electronic states are not completely orthogonal, the optimized excited states can contain noticeable undesirable admixtures of the lower-lying states of the same symmetry. To produce orthogonal electronic states without strictly enforcing the orthogonality constraint, the interstate penalty strength is gradually increased using a fixed multiplicative update factor  $f_{upd} > 1$

$$C_P^{(n+1)} = C_P^{(n)} \times f_{upd} \quad (14)$$

until the electronic states become orthogonal, that is, until the deviation from the orthogonality (DFO) measured by the max norm of the off-diagonal elements of the interstate overlap matrix drops below a user-specified threshold  $\mathcal{E}_0$ :

$$\text{DFO} \equiv \|\Phi_{\tau d}^{-1/2} \Phi_{\tau} \Phi_{\tau d}^{-1/2} - I\|_{\max} < \mathcal{E}_0 \quad (15)$$

$C_P$  is adjusted in the outer loop, each iteration of which runs the PCG optimizer with a fixed penalty strength. This procedure guarantees that the optimization does not only produces accurate fully optimized MOs for each state, but also enforces orthogonality between the electronic states.

**Computational details.** The VM TIDFT procedure was implemented in the electronic structure module of the CP2K software package<sup>61</sup>. In the current implementation, matrix operations were performed using the DBCSR<sup>62</sup> library for sparse matrices and ScaLAPACK<sup>63</sup> library for dense matrices. The default values for the input parameters that control convergence of the PCG VM optimization are shown in Table 1 and used unless specified otherwise.

The efficiency and accuracy of the VM TIDFT method was tested on systems including gas-phase atoms (He, Be, B, Li) and small molecules (azulene, benzene, butadiene, ethene, formaldehyde, hydrogen chloride, hydrogen fluoride, nitrobenzene, N-phenylpyrrole, pyrrole, pyrazine, and naphthalene). We also calculated excitations in molecular complexes  $\text{C}_2\text{H}_4 \dots \text{C}_2\text{F}_4$ ,  $\text{NH}_3\text{-BF}_3$ ,  $\text{NH}_3 \dots \text{F}_2$ , and  $\pi$ -stacked dimer of pyrrole and pyrazine molecules. The organic molecules, particularly azulene, benzene, butadiene, nitrobenzene, and N-phenylpyrrole, are of special interest due to their distinct excited-state behavior driven by CT and bonding-antibonding inter-

Parameter	Notation	Default value	Described in
Initial interstate penalty strength	$C_P^{(0)}$	10 Ha	Eq. (14)
SCF convergence threshold	$\ \frac{\partial \Omega}{\partial T}\ _{\text{RMS}}$	$10^{-6}$ Ha	
Final allowed DFO	$\mathcal{E}_0$	$10^{-3}$	Eq. (15)
Interstate update factor	$f_{\text{upd}}$	2	Eq. (14)
Hamiltonian term in the preconditioner	$A$	0	Eq. (13) and Ref. <sup>54</sup>
Overlap term in the preconditioner	$D$	$I$	Eq. (13) and Ref. <sup>54</sup>

TABLE 1. Input parameters that control the PCG optimization of MO coefficients.

actions. These conjugated systems, with near-degenerate core and delocalized  $\pi$ -orbitals, are prone to root-flipping issues<sup>64,65</sup> during excited-state calculations, complicating the identification of states and making them excellent benchmarks. Moreover, the availability of extensive experimental and computational data for these systems enables meaningful comparisons, ensuring the reliability and accuracy of the tested method.

Unrestricted Kohn-Sham formalism (UKS) was used to describe spin-orbitals in this study unless indicated otherwise. Test calculations were carried out using the generalized gradient exchange-correlation functional of Perdew, Burke and Ernzerhof (PBE)<sup>66–68</sup>. In the dual Gaussian and plane-wave scheme implemented in CP2K<sup>69</sup>, double- $\zeta$  valence basis set with one set of polarization functions (DZVP)<sup>70</sup> were used to represent atomic orbitals. A plane-wave cutoff of 300 Ry was established to adequately describe the electron density, whereas a higher cutoff of 1500 Ry was used to produce smooth dissociation curves for the hydrogen  $H_2$  and the  $\text{HeH}^+$  molecules. Separable norm-conserving Goedecker-Teter-Hutter pseudopotentials were used to describe the interactions between the valence electrons and ionic cores<sup>71,72</sup>. All calculations were performed using a cubic simulation cell with dimensions of  $15 \times 15 \times 15$  for  $H_2$  and  $30 \times 30 \times 30$  for the rest of the systems. Electrostatic interactions between the periodic cell was eliminated using wavelet approach<sup>73,74</sup>.

## DATA AVAILABILITY

Optimized atomic coordinates for all structures and lattice vectors are deposited in a Figshare database.

## RESULTS AND DISCUSSION

**Penalty strength effect.** Fig. 1 shows the impact of the residual nonorthogonality between electronic states on the excitation energies. With higher penalty strength  $C_P$ , the electronic states are pushed to become orthogonal decreasing DFO and recovering the true excitation energies. When the allowed DFO is too large, only a

fraction of the true excitation energies is recovered, signalling the admixture of lower-lying states due to insufficient orthogonality enforcement. This data highlights the importance of the interstate penalty term and suggests that  $\mathcal{E}_0 = 10^{-4}$  is an acceptable DFO that recovers a large fraction of excitation energies. For HF, the bonding interaction arises from the overlap between the hydrogen 1s orbital and the fluorine  $2p_z$  orbital, while the  $1\pi$  orbitals are non-bonding as they have wrong symmetry to interact with the H 1s orbital and are localized primarily on the fluorine atom.

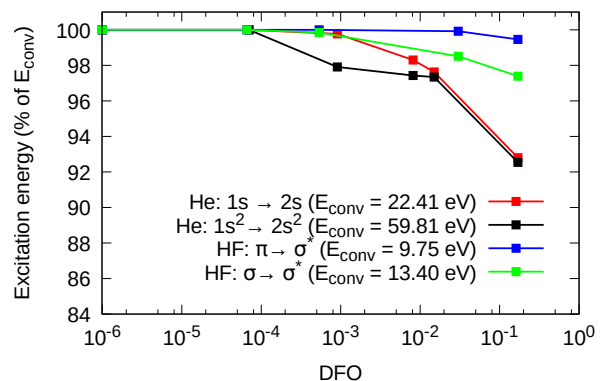


FIG. 1. Excitation energy for the first two excitations of He atom (PBE/TZVP) and HF molecule (PBE/DZVP) computed with VM TIDFT optimization procedure for the DFO values measured after convergence is reached. The recovered excitation energy is a fraction of the converged excitation energy  $E_{\text{conv}}$  obtained with very tight requirement for the orthogonality criterion ( $\mathcal{E}_0 = 10^{-5}$ ).

**Accuracy.** Table 3 compares experimentally measured first singlet excitation energies with those computed using VM TIDFT, TDDFT in Tamm-Dancoff approximation, OCDFT, and wavefunction-based correlation methods (MP2 or CCSD).

Despite different optimization paradigms, VM TIDFT utilizes the same orthogonality constraint as OCDFT. Therefore, the fully optimized states in VM TIDFT and OCDFT are expected to be the same if computed using the same model chemistry (i.e. the same exchange-

correlation functional and basis set). Table 3 shows that VM TIDFT excitation energies are indeed close to those computed with OCDFT but not the same. This is due to the OCDFT results being partially spin-purified in the post-SCF procedure<sup>32</sup>, whereas spin-purification was not used in VM TIDFT optimization. The results are also different due to the different basis sets employed to represent occupied states: def2-TZVP in OCDFT is a larger more flexible basis set than DZVP in VM TIDFT.

For the six systems with complete experimental and computational data (first six rows in Table 3), VM TIDFT results are in reasonable agreement with experimental data (MAD = 1.02 eV). For comparison, the partially spin-purified OCDFT results are in slightly better agreement with experimental data than VM TIDFT (MAD = 0.89 eV), whereas TDDFT agreement is significantly worse (MAD = 1.71 eV).

When all test systems with available experimental excitation energies, are compared (not just the first six of them), the accuracy of VM TIDFT (MAD = 0.88 eV) remains noticeably better than that of TDDFT (MAD = 1.36 eV). Comparison between VM TIDFT and TDDFT shows that TDDFT tends to slightly underestimate excitation energies for the test systems (Fig. 2). On the other hand, VM TIDFT energies are underestimated compared to OCDFT, MP2, and CCSD energies (Fig. 2). OCDFT data suggests that using spin-purified VM TIDFT wavefunctions, described with larger basis set can substantially improve the excitation energies. Spin-purified VM TIDFT calculations will be performed using the ROKS optimizer in the future.

It is worth noting the magnitude of the residual norm of the energy gradient for the fully optimized excited states (Table 3). For most excited states, this norm is below the convergence threshold of  $10^{-6}$  Ha imposed on the loss (not the energy) functional, indicating that these excited states are true minima of the DFT functional. Once optimized, these states will not collapse to the lower lying ground state even without the orthogonality constraint. There are, however, several excited systems with the energy gradient higher than the  $10^{-6}$  Ha threshold. These are He atom, N-phenylpyrrole,  $\text{NH}_3 \dots \text{BF}_3$ , and pyrrole-pyrazine dimer. In these systems, the first excited states are not electronic minima and, in these optimized states, the non-zero energy gradient is fully compensated by the opposite non-zero gradient of the interstate penalty functional, producing the zero-gradient true minima of the loss functional. It is also important to note that such stationary points still correspond to physically meaningful excited states<sup>75</sup>. For instance, VM TIDFT results for the He atom match closely TDDFT results and experimental data for low-lying excitations while not being true electronic minima (Table 2). This confirms the validity of using orthogonality constraints in orbital-optimized excited-state DFT.

**Double-electron excitations.** Unlike TDDFT, VM

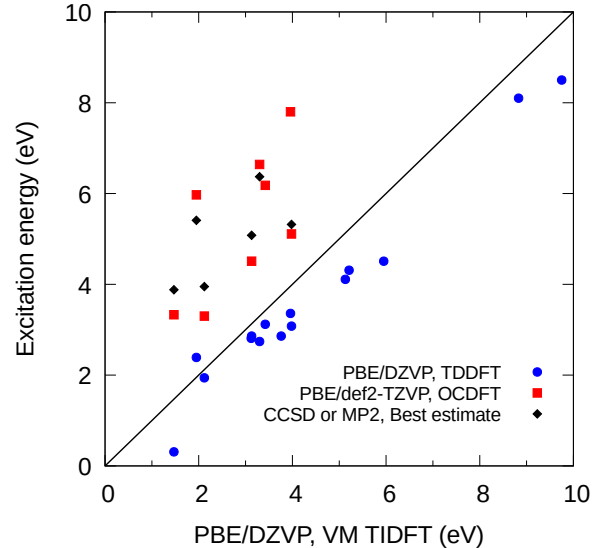


FIG. 2. Comparison of VM TIDFT excitation energies with those calculated with TDDFT, OCDFT, and wavefunction correlation methods. TDDFT and VM TIDFT results were obtained in this work using CP2K, OCDFT energies were computed using Psi4 in Ref.<sup>32</sup>, and MP2/6-31G\* and CCSD/aug-cc-pVTZ results were computed using Gaussian in Ref.<sup>79</sup>.

TIDFT can trivially describe double-electron excitations. As an example, the energies calculated for the  $1s^2 \rightarrow 2s^2$  and  $1s^2 \rightarrow 2s^1 2p^1$  excitations in the helium atom are 57.68 eV and 67.63 eV, respectively, at the PBE/QZV3P level of theory. These values are close to the experimental values for these transitions, which are 57.84 eV<sup>77</sup> and 60.15 eV<sup>78</sup>, respectively. It should be noted that OCDFT with a single electron hole-particle pair cannot describe double-electron excitations<sup>32</sup>.

**Charge-transfer excitations.** One of the most important advantages of OODFT methods over TDDFT is their ability to predict the energy of CT excitations accurately. Here, VM TIDFT is used to describe the CT excitation in a minimal-basis  $\text{H}_2$  molecule – a simple four-level test system previously employed to explain the success of OCDFT and failures of TDDFT<sup>32</sup>. Fig. 3 shows that VM TIDFT indeed correctly reproduces the long-range behavior of the CT excitation energy, matching the Coulomb potential of the interacting  $\text{H}^+$  and  $\text{H}^-$  ions perfectly. This behavior can be contrasted with the TDDFT CT energy of the excited states, which shows the attenuation of the Coulomb tail<sup>32</sup>, the degree of which is determined by the fraction of the exact exchange in the employed exchange functional.

It is also instructive to demonstrate the correct behavior of the CT excitation energies in the  $[\text{He} \dots \text{H}]^+$  ion. For large interatomic distances, the two electrons in the  $[\text{He} \dots \text{H}]^+$  system are localized on the helium atom in the

Excitation	RMS norm of the			
	TDDFT (eV)	VM TIDFT (eV)	energy gradient (Ha)	Experiment (eV)
$1s^2 \rightarrow 1s2s$	17.48	20.27	$7.9 \times 10^{-2}$	20.62 <sup>76</sup>
$1s^2 \rightarrow 1s2p$	21.07	22.17	$9.1 \times 10^{-7}$	21.22 <sup>76</sup>
$1s^2 \rightarrow 1s3s$	30.87	29.52	$1.9 \times 10^{-2}$	22.93 <sup>76</sup>
$1s^2 \rightarrow 2s^2$	-	58.09	$4.3 \times 10^{-1}$	57.84 <sup>77</sup>
$1s^2 \rightarrow 2s2p$	-	65.79	$3.9 \times 10^{-1}$	60.15 <sup>78</sup>

TABLE 2. PBE/aug-cc-pV5Z excitation energies calculated using TDDFT and VM TIDFT with  $\epsilon_0 = 10^{-5}$ .

Molecules	RMS norm of the energy gradient (Ha)	CP2K		Psi4	Gaussian	Experiment (eV)
		PBE/DZVP		PBE/def2-TZVP	MP2/6-31G*	
		TDDFT (eV)	VM TIDFT (eV)	OCDFT <sup>32</sup> (eV)	CCSD/aug-cc-pVTZ Best estimate <sup>79</sup> (eV)	
pyrazine	$6.0 \times 10^{-7}$	2.86	3.13	3.30	3.95 <sup>a</sup>	3.83 <sup>80</sup>
formaldehyde	$8.4 \times 10^{-7}$	3.12	3.42	3.33	3.88 <sup>a</sup>	4.28 <sup>81</sup>
benzene	$9.9 \times 10^{-7}$	4.11	5.13	5.11	5.08 <sup>a</sup>	4.79 <sup>82</sup>
pyrrole	$7.8 \times 10^{-7}$	4.31	5.21	5.97	6.37 <sup>a</sup>	5.22 <sup>83</sup>
butadiene	$7.3 \times 10^{-7}$	2.86	3.76	4.51	6.18 <sup>a</sup>	5.92 <sup>84</sup>
ethene	$4.9 \times 10^{-7}$	4.51	5.95	6.64	7.80 <sup>a</sup>	8.00 <sup>84</sup>
azulene	$8.9 \times 10^{-7}$	1.94	2.12	-	3.85 <sup>b</sup>	1.77 <sup>85</sup>
B atom	$5.9 \times 10^{-7}$	0.31	1.47	-	-	1.86 <sup>86</sup>
Be atom	$5.5 \times 10^{-7}$	3.08	3.98	-	-	2.73 <sup>87</sup>
Li atom	$7.2 \times 10^{-7}$	2.39	1.95	-	-	3.37 <sup>88</sup>
naphthalene	$9.1 \times 10^{-7}$	2.74	3.30	-	-	3.97 <sup>89</sup>
N-phenylpyrrole	$4.2 \times 10^{-3}$	3.36	3.96	-	5.32 <sup>b</sup>	4.35 <sup>90</sup>
nitrobenzene	$8.9 \times 10^{-7}$	2.81	3.12	-	5.41 <sup>b</sup>	4.38 <sup>91</sup>
HCl	$8.8 \times 10^{-7}$	8.10	8.83	-	-	9.56 <sup>92</sup>
HF	$6.2 \times 10^{-7}$	8.50	9.75	-	-	10.33 <sup>93</sup>
He atom	$1.9 \times 10^{-1}$	24.15	26.03	-	-	20.62 <sup>76</sup>
NH <sub>3</sub> ...F <sub>2</sub>	$9.1 \times 10^{-7}$	1.90	2.50	-	-	-
pyrrole...pyrazine	$1.8 \times 10^{-6}$	2.52	3.10	-	-	-
C <sub>2</sub> H <sub>4</sub> ...C <sub>2</sub> F <sub>4</sub>	$5.8 \times 10^{-7}$	4.39	5.46	-	-	-
NH <sub>3</sub> -BF <sub>3</sub>	$1.8 \times 10^{-4}$	7.29	8.81	-	-	-
MAE vs Experiment <sup>c</sup>		1.71	1.02	0.89	0.52	0.00
MAE vs Experiment <sup>d</sup>		1.36	0.88	-	-	0.00

<sup>a</sup> MP2/6-31G(d) results<sup>79</sup>

<sup>b</sup> CCSD/aug-cc-pVTZ results<sup>79</sup>

<sup>c</sup> Computed for the first six systems

<sup>d</sup> Computed for the systems with listed experimental values

TABLE 3. First singlet excitation energies calculated using TDDFT, VM TIDFT, OCDFT and high-level quantum mechanics calculations and shown alongside experimental data.

ground state. Upon excitation, one of the electrons transfers from helium to hydrogen, resulting in a  $\text{He}^+ \dots \text{H}$  configuration. The energy of this excitation is the sum of the ionization potential (IP) of helium and the electron

affinity (EA) of hydrogen. Crucially, this energy does not depend on the interatomic distance because the Coulomb interaction between the neutral and positive fragments is zero. VM TIDFT correctly reproduces the flat excitation

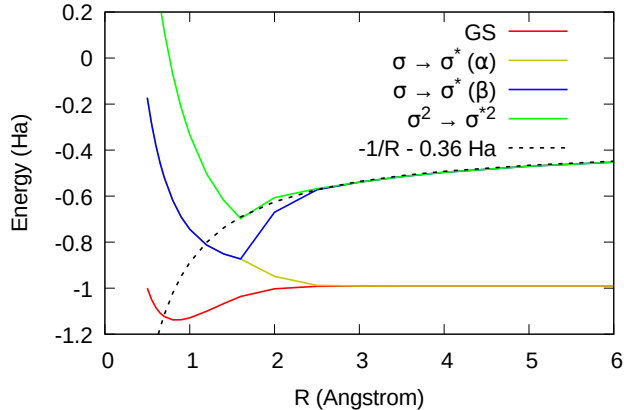


FIG. 3. PBE/SZV ground-state and excited-state dissociation curves for  $H_2$  computed with VM TIDFT. The energy of the Coulomb interactions is down-shifted by 0.36 Ha to account for sum of the ionization potential (IP) and electron affinity (EA) of the isolated hydrogen atoms.

energy in the large separation limit, in agreement with the spin-purified OCDFT excitation energy (Fig. 4). In contrast, TDDFT underestimates the excitation energy and fails to capture its asymptotic behavior (Fig. 4) because of the incomplete cancellation of the Coulomb and exchange interactions between electrons in the PBE and other exchange-correlation functionals.

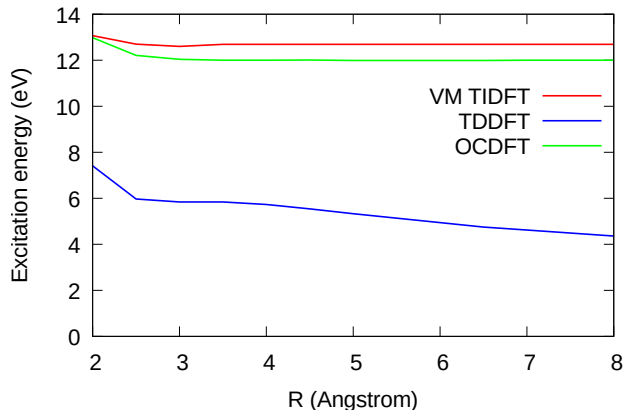


FIG. 4. Excitation energy for the charge transfer state of  $HeH^+$  as a function of the He-H distance, computed using VM TIDFT and TDDFT at the PBE/DZVP level of theory. For comparison, OCDFT PBE/STO-3G results are also shown<sup>32</sup>.

**SCF convergence.** Fig. 5 shows how the norm of the gradient of the loss functional changes during the PCG optimization of the ground and excited states. The default VM SCF optimization algorithm achieves stable convergence for the ground state<sup>54</sup>. The algorithm also works well for the optimization of excited-state orbitals,

sometimes converging faster than the optimization of the ground state. This is because an excited-state optimization already starts with the well-converged canonical orbitals of the ground state. For some systems, however, the optimization of the excited states takes many more iterations to converge as the optimizer needs to find the right balance between maintaining orthogonality to the previously optimized states and minimizing the energy. Converging excited-state optimization also takes longer when the penalty strength update is necessary to enforce stricter orthogonality between the electronic states. These updates, performed in an outer loop of the main PCG optimization, can be seen as sharp increases of the gradient norm from the convergence line in Fig. 5.

It should be noted that a large number of iterations is required to achieve convergence even for the ground state of simple systems. This suggests that the rate of convergence can be improved by replacing PCG – one of the simplest algorithms for unconstrained optimization – with quasi-Newton or trust-region optimizers that are known to work well for the ground-state KS DFT<sup>50</sup>. Additionally, faster optimization can be achieved by updating the penalty strength on each iteration, instead of updating it in the outer loop.

Finally, it is worth mentioning that VM TIDFT method does not guarantee to find the lowest-energy excitations. As with all other orbital-optimized DFT methods<sup>6</sup>, the result of the optimization will be a stationary point lying in the basin of the initial guess.

## CONCLUSIONS

VM TIDFT is a simple DFT method designed to prevent collapse of excited states during their variational optimization. The main idea of VM TIDFT is to allow nonorthogonal electronic states in the optimization process but gradually push them towards orthogonality with a simple continuous penalty function. With nonorthogonal orbitals and electronic states, VM TIDFT can use molecular orbital coefficients as independent variables in the optimization procedure. This in turn leads to simple closed-form analytical expressions for the gradient and allows to employ any of the ubiquitous unconstrained optimization algorithms that guarantees convergence of the excited-state optimization. Numerical tests on multiple molecular systems show that VM TIDFT optimization performed with the PCG algorithm is robust and the method computes accurate energies for well-behaved excitations and, unlike TDDFT, for more challenging CT and double-electron excitations.

Due to the simplicity of VM TIDFT, this approach can be implemented using other unconstrained minimization techniques, such as quasi-Newton or trust-region methods. This can improve the computational efficiency of VM DFT. VM TIDFT is also ideally suited to imple-



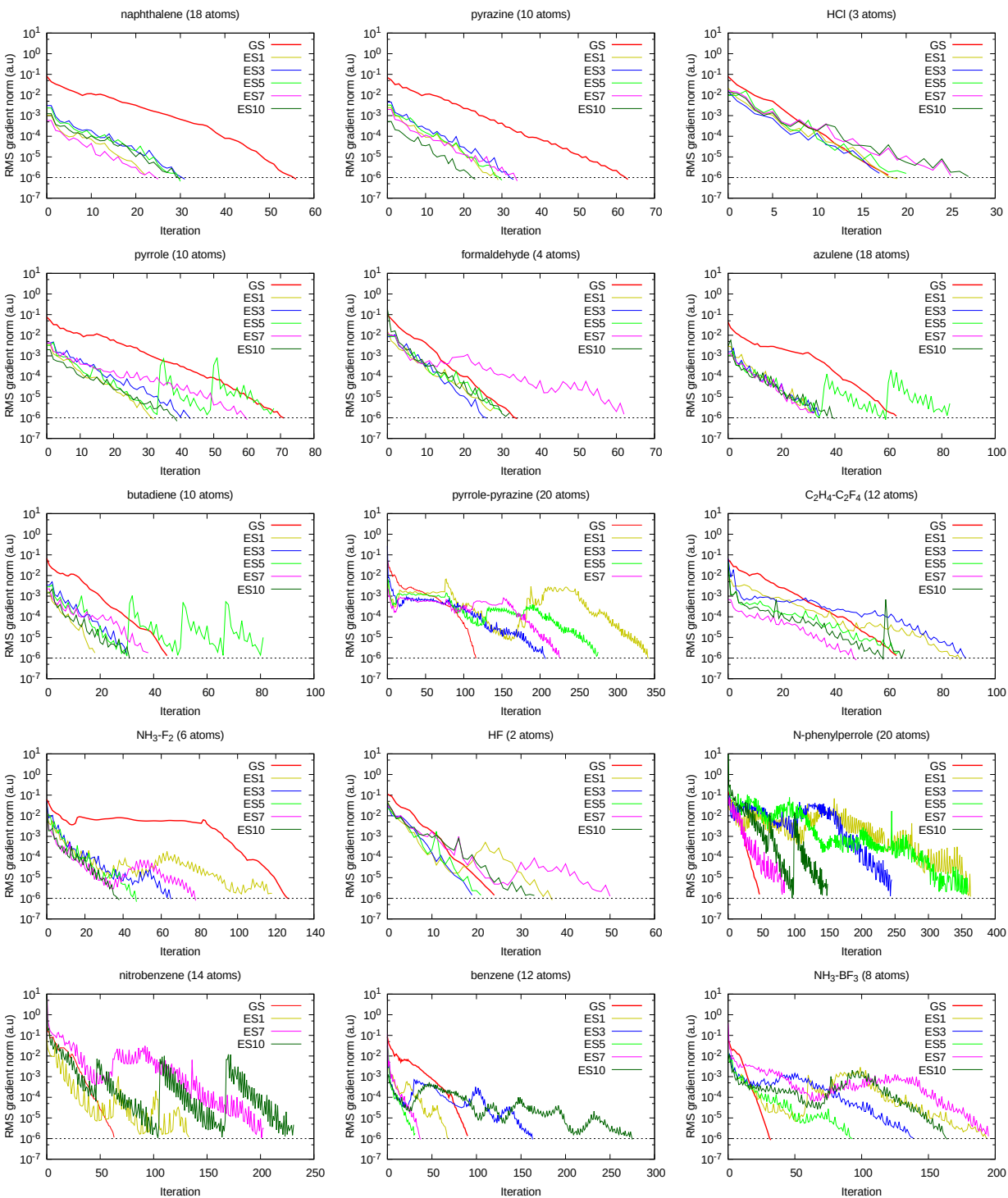


FIG. 5. Convergence rate for the VM TIDFT procedure for the ground states (GS) and selected excited states (ES). Line search steps, one per PCG step, are not included in the iteration count. The dashed lines show the SCF convergence threshold.

ment the full variational ROKS optimization of spin-purified open-shell singlet states<sup>54–56</sup>, which are necessary for more accurate description of many excited states. Additionally, unconstrained VM TIDFT optimization makes the computation of atomic forces in ex-

cited states straightforward, facilitating computation of emission spectra and dynamical photophysical and photochemical processes in excited states.

From a broader perspective, variable-metric optimization can be readily extended to electronic structure meth-

ods where the use of nonorthogonal wavefunctions is unavoidable (e.g. optimization of strictly localized orbitals<sup>94–97</sup>), or where linear dependencies present a serious problem during variational optimization (e.g. multi-configurational wavefunctions).

## ACKNOWLEDGEMENTS

We would like to thank Zhenzhe Zhang for providing optimized structures for our tests. The research was funded by the Natural Sciences and Engineering Research Council of Canada (NSERC) through Discovery Grant. The authors are grateful to Compute Canada for computer resources allocated under the CFI John R. Evans Leaders Fund program.

- 
- (1) Matsika, S.; Krylov, A. I. Introduction: Theoretical Modeling of Excited State Processes. *Chem. Rev* **2017**, *117*, 49.
  - (2) Serrano-Andrés, L.; Merchán, M. Quantum chemistry of the excited state: 2005 overview. *J. Mol. Struct. Theochem.* **2005**, *729*, 99–108.
  - (3) Schlag, E. W.; Schneider, S.; Fischer, S. F. Lifetimes in Excited States. *Annu. Rev. Phys. Chem.* **1971**, *22*, 465–526.
  - (4) Dreuw, A.; Head-Gordon, M. Single-reference ab initio methods for the calculation of excited states of large molecules. *Chem. Rev.* **2005**, *105*, 4009–4037.
  - (5) Runge, E.; Gross, E. K. Density-Functional Theory for Time-Dependent Systems. *Phys. Rev. Letters* **1984**, *52*, 997.
  - (6) Hait, D.; Head-Gordon, M. Orbital Optimized Density Functional Theory for Electronic Excited States. *J. Phys. Chem. Lett.* **2021**, *12*, 4517–4529.
  - (7) Ullrich, C. A. *Time-Dependent Density-Functional Theory: Concepts and Applications*; Oxford University Press, 2011.
  - (8) Levy, M.; Ágnes Nagy Variational density-functional theory for an individual excited state. *Phys. Rev. Lett.* **1999**, *83*, 4361.
  - (9) Nagy, M.; Levy, M. Variational density-functional theory for degenerate excited states. *Phys. Rev. A: At. Mol. Opt. Phys.* **2001**, *63*, 052502.
  - (10) Ayers, P. W.; Levy, M. Time-independent (static) density-functional theories for pure excited states: Extensions and unification. *Phys. Rev. A* **2009**, *80*, 012508.
  - (11) Ayers, P. W.; Levy, M.; Nagy, A. Time-independent density-functional theory for excited states of Coulomb systems. *Phys. Rev. A* **2012**, *85*, 042518.
  - (12) Cullen, J.; Krykunov, M.; Ziegler, T. The formulation of a self-consistent constricted variational density functional theory for the description of excited states. *Chem. Phys.* **2011**, *391*, 124107.
  - (13) Ziegler, T.; Rauk, A.; Baerends, E. J. On the calculation of multiplet energies by the hartree-fock-slater method. *Theor. Chim. Acta.* **1977**, *43*, 261–271.
  - (14) Barth, U. V. Local-density theory of multiplet structure. *Phys. Rev. A* **1979**, *20*, 1693–1703.
  - (15) Gavnholt, J.; Olsen, T.; Engelund, M.; Schiøtz, J.  $\Delta$  self-consistent field method to obtain potential energy surfaces of excited molecules on surfaces. *Phys. Rev. B - Condens. Matter Phys* **2008**, *78*, 075441.
  - (16) Kowalczyk, T.; Yost, S. R.; Voorhis, T. V. Assessment of the  $\Delta$ SCF Density Functional Theory Approach for Electronic Excitations in Organic Dyes. *J. Chem. Phys.* **2011**, *134*, 054128.
  - (17) Yang, W.; Ayers, P. W. Foundation for the  $\Delta$ SCF Approach in Density Functional Theory. 2024; <https://arxiv.org/abs/2403.04604>.
  - (18) Triguero, L.; Plashkevych, O.; Pettersson, L. G.; Ågren, H. Separate state vs. transition state Kohn-Sham calculations of X-ray photoelectron binding energies and chemical shifts. *J. Electron Spectros. Relat. Phenom.* **1999**, *104*, 195–207.
  - (19) Cheng, C. L.; Wu, Q.; Voorhis, T. V. Rydberg energies using excited state density functional theory. *J. Chem. Phys.* **2008**, *129*, 124112.
  - (20) Seidu, I.; Krykunov, M.; Ziegler, T. Applications of time-dependent and time-independent density functional theory to Rydberg transitions. *J. Phys. Chem. A* **2015**, *119*, 5107–5116.
  - (21) Liu, J.; Zhang, Y.; Bao, P.; Yi, Y. Evaluating Electronic Couplings for Excited State Charge Transfer Based on Maximum Occupation Method  $\Delta$ SCF Quasi-Adiabatic States. *J. Chem. Theory Comput.* **2017**, *13*, 843–851.
  - (22) Hait, D.; Head-Gordon, M. Highly Accurate Prediction of Core Spectra of Molecules at Density Functional Theory Cost: Attaining Sub-electronvolt Error from a Restricted Open-Shell Kohn-Sham Approach. *J. Phys. Chem. Lett.* **2020**, *11*, 775–786.
  - (23) Kumar, C.; Luber, S. Robust  $\Delta$ SCF calculations with direct energy functional minimization methods and STEP for molecules and materials. *J. Chem. Phys.* **2022**, *156*, 154104.
  - (24) Selenius, E.; Sigurdarson, A. E.; Schmerwitz, Y. L. A.; Levi, G. Orbital-Optimized Versus Time-Dependent Density Functional Calculations of Intramolecular Charge Transfer Excited States. *J. Chem. Theory Comput.* **2024**, *20*, 3809–3822.
  - (25) Kunze, L.; Hansen, A.; Grimme, S.; Mewes, J. M. PCMRKS for the Description of Charge-Transfer States in Solution: Singlet-Triplet Gaps with Chemical Accuracy from Open-Shell Kohn-Sham Reaction-Field Calculations. *J. Phys. Chem. Lett.* **2021**, *12*, 8470–8480.
  - (26) Nottoli, M.; Mazzeo, P.; Lipparini, F.; Cupellini, L.; Mennucci, B. A  $\Delta$ SCF model for excited states within a polarisable embedding. *Mol. Phys.* **2023**, *121*, e2089605.
  - (27) Gross, E. K.; Oliveira, L. N.; Kohn, W. Density-functional theory for ensembles of fractionally occupied states. I. Basic formalism. *Phys. Rev. A* **1988**, *37*, 2821.
  - (28) Gilbert, A. T.; Besley, N. A.; Gill, P. M. Self-consistent field calculations of excited states using the maximum overlap method (MOM). *J. Phys. Chem. A* **2008**, *112*, 13164–13171.
  - (29) Baruah, T.; Pederson, M. R. DFT calculations on charge-transfer states of a carotenoid-porphyrin-C60 molecular triad. *J. Chem. Theory Comput.* **2009**, *5*, 834–843.
  - (30) Kaduk, B.; Kowalczyk, T.; Voorhis, T. V. Constrained density functional theory. *Chem. Rev.* **2012**, *112*, 321–

- 370.
- (31) Ziegler, T.; Krykunov, M.; Cullen, J. The implementation of a self-consistent constricted variational density functional theory for the description of excited states. *J. Chem. Phys.* **2012**, *136*, 124107.
- (32) Evangelista, F. A.; Shushkov, P.; Tully, J. C. Orthogonality Constrained Density Functional Theory for Electronic Excited States. *J. Phys. Chem. A* **2013**, *117*, 7378–7392.
- (33) Filatov, M. Spin-restricted ensemble-referenced Kohn-Sham method: Basic principles and application to strongly correlated ground and excited states of molecules. *Wiley Interdiscip. Rev. Comput. Mol. Sci.* **2015**, *5*, 146–167.
- (34) Ramos, P.; Pavanello, M. Low-lying excited states by constrained DFT. *J. Chem. Phys.* **2018**, *148*, 144103.
- (35) Levi, G.; Ivanov, A. V.; Jónsson, H. Variational Density Functional Calculations of Excited States via Direct Optimization. *J. Chem. Theory Comput.* **2020**, *16*, 6968–6982.
- (36) Levi, G.; Ivanov, A. V.; Jónsson, H. Variational Calculations of Excited States: Via Direct Optimization of the Orbitals in DFT. *Faraday Discuss.* **2020**, *224*, 448–466.
- (37) Zhao, L.; Neuscamman, E. Density Functional Extension to Excited-State Mean-Field Theory. *J. Chem. Theory Comput.* **2020**, *16*, 164–178.
- (38) Carter-Fenk, K.; Herbert, J. M. State-Targeted Energy Projection: A Simple and Robust Approach to Orbital Relaxation of Non-Aufbau Self-Consistent Field Solutions. *J. Chem. Theory Comput.* **2020**, *16*, 5067–5082.
- (39) Hait, D.; Head-Gordon, M. Excited State Orbital Optimization via Minimizing the Square of the Gradient: General Approach and Application to Singly and Doubly Excited States via Density Functional Theory. *J. Chem. Theory Comput.* **2020**, *16*, 1699–1710.
- (40) Roychoudhury, S.; Sanvito, S.; O’Regan, D. D. Neutral excitation density-functional theory: an efficient and variational first-principles method for simulating neutral excitations in molecules. *Sci. Rep.* **2020**, *10*, 8947.
- (41) Ivanov, A. V.; Levi, G.; Jónsson, E.; Jónsson, H. Method for Calculating Excited Electronic States Using Density Functionals and Direct Orbital Optimization with Real Space Grid or Plane-Wave Basis Set. *J. Chem. Theory Comput.* **2021**, *17*, 5034–5049.
- (42) MacEtti, G.; Genoni, A. Initial maximum overlap method for large systems by the quantum mechanics/extremely localized molecular orbital embedding technique. *J. Chem. Theory Comput.* **2021**, *17*, 4169–4182.
- (43) Zhang, J.; Tang, Z.; Zhang, X.; Zhu, H.; Zhao, R.; Lu, Y.; Gao, J. Target State Optimized Density Functional Theory for Electronic Excited and Diabatic States. *J. Chem. Theory Comput.* **2023**, *19*, 1777–1789.
- (44) Schmerwitz, Y. L. A.; Levi, G.; Jónsson, H. Calculations of Excited Electronic States by Converging on Saddle Points Using Generalized Mode Following. *J. Chem. Theory Comput.* **2023**, *19*, 3651.
- (45) Ziegler, T.; Krykunov, M.; Seidu, I.; Park, Y. C. In *Constricted variational density functional theory approach to the description of excited states*; Michael, Nicolas, H.-R. M. F., Filatov, Eds.; Springer International Publishing, 2015; Vol. 368; pp 61–95.
- (46) Cernatic, F.; Senjean, B.; Robert, V.; Fromager, E. Ensemble Density Functional Theory of Neutral and Charged Excitations: Exact Formulations, Standard Approximations, and Open Questions. *Top. Curr. Chem. (Z)* **2022**, *380*, 4.
- (47) Barca, G. M.; Gilbert, A. T.; Gill, P. M. Simple Models for Difficult Electronic Excitations. *J. Chem. Theory Comput.* **2018**, *14*, 1501–1509.
- (48) Barca, G. M.; Gilbert, A. T.; Gill, P. M. Excitation Number: Characterizing Multiply Excited States. *J. Chem. Theory Comput.* **2018**, *14*, 9–13.
- (49) Mewes, J. M.; Jovanović, V.; Marian, C. M.; Dreuw, A. On the molecular mechanism of non-radiative decay of nitrobenzene and the unforeseen challenges this simple molecule holds for electronic structure theory. *Phys. Chem. Chem. Phys.* **2014**, *16*, 12393–12406.
- (50) Voorhis, T. V.; Head-Gordon, M. A geometric approach to direct minimization. *Mol. Phys.* **2002**, *100*, 1713–1721.
- (51) Shea, J. A.; Gwin, E.; Neuscamman, E. A Generalized Variational Principle with Applications to Excited State Mean Field Theory. *J. Chem. Theory Comput.* **2020**, *16*, 1526–1540.
- (52) Luo, Z.; Khaliullin, R. Z. Direct Unconstrained Variable-Metric Localization of One-Electron Orbitals. *J. Chem. Theory Comput.* **2020**, *16*, 3558–3566.
- (53) Luo, Z.; Khaliullin, R. Z. Variable-Metric Localization of Occupied and Virtual Orbitals. *J. Chem. Theory Comput.* **2021**, *17*, 5581.
- (54) Pham, H. D. M.; Khaliullin, R. Z. Direct Unconstrained Optimization of Molecular Orbital Coefficients in Density Functional Theory. *J. Chem. Theory Comput.* **2024**, *20*, 7936–7947.
- (55) Frank, I.; Hutter, J.; Marx, D.; Parrinello, M. Molecular dynamics in low-spin excited states. *J. Chem. Phys.* **1998**, *108*, 164101.
- (56) Filatov, M.; Shaik, S. Density-functional thermochemistry. III. The role of exact exchange. *J. Chem. Phys.* **1999**, *110*, 5648.
- (57) Nocedal, J.; Wright, S. J. *Numerical Optimization*, 2nd ed.; Springer: New York, NY, USA, 2006.
- (58) A Survey of Nonlinear Conjugate Gradient Methods. *Pac. J. Optim.* **2006**, *2*, 35–58.
- (59) Stewart, G. W. On the adjugate matrix. *Linear Algebra Its Appl.* **1998**, *283*, 151–164.
- (60) VandeVondele, J.; Hutter, J. An efficient orbital transformation method for electronic structure calculations. *J. Chem. Phys.* **2003**, *118*, 4365.
- (61) Kühne, T. D. et al. CP2K: An Electronic Structure and Molecular Dynamics Software Package -Quickstep: Efficient and Accurate Electronic Structure Calculations. *J. Chem. Phys.* **2020**, *152*, 194103.
- (62) Borštnik, U.; VandeVondele, J.; Weber, V.; Hutter, J. Sparse matrix multiplication: The distributed block-compressed sparse row library. *Parallel Comp.* **2014**, *40*, 47–58.
- (63) Choi, J.; Demmel, J.; Dhillon, I.; Dongarra, J.; Ostrouchov, S.; Petitet, A.; Stanley, K.; Walker, D.; Whaley, R. ScaLAPACK: a portable linear algebra library for distributed memory computers — design issues and performance. *Comput. Phys. Commun.* **1996**, *97*, 1–15.
- (64) Marie, A.; Burton, H. G. Excited States, Symmetry Breaking, and Unphysical Solutions in State-Specific CASSCF Theory. *J. Phys. Chem. A* **2023**, *127*, 4538–4552.

- (65) Tran, L. N.; Shea, J. A.; Neuscammann, E. Tracking Excited States in Wave Function Optimization Using Density Matrices and Variational Principles. *J. Chem. Theory Comput.* **2019**, *15*, 4790–4803.
- (66) Zhang, Y.; Yang, W. Comment on “Generalized Gradient Approximation Made Simple”. *Phys. Rev. Lett.* **1998**, *80*, 890–890.
- (67) Perdew, J. P.; Ruzsinszky, A.; Csonka, G. I.; Vydrov, O. A.; Scuseria, G. E.; Constantin, L. A.; Zhou, X.; Burke, K. Restoring the density-gradient expansion for exchange in solids and surfaces. *Phys. Rev. Lett.* **2008**, *100*, 136406.
- (68) Perdew, J. P.; Burke, K.; Ernzerhof, M. Generalized Gradient Approximation Made Simple [Phys. Rev. Lett. 77, 3865 (1996)]. *Phys. Rev. Lett.* **1997**, *78*, 1396–1396.
- (69) Hutter, J.; Iannuzzi, M.; Schiffmann, F.; Vandevondele, J. Cp2k: Atomistic Simulations of Condensed Matter Systems. *Wiley Interdiscip. Rev. Comput. Mol. Sci.* **2014**, *4*, 15–25.
- (70) VandeVondele, J.; Hutter, J. Gaussian Basis Sets for Accurate Calculations on Molecular Systems in Gas and Condensed Phases. *J. Chem. Phys.* **2007**, *127*, 114105.
- (71) Goedecker, S.; Teter, M.; Hutter, J. Separable Dual-Space Gaussian Pseudopotentials. *Phys. Rev. B* **1996**, *54*, 1703.
- (72) Krack, M. Pseudopotentials for H to Kr Optimized for Gradient-Corrected Exchange-Correlation Functionals. *Theor. Chem. Acc.* **2005**, *114*, 145–152.
- (73) Genovese, L.; Deutsch, T.; Neelov, A.; Goedecker, S.; Beylkin, G. Efficient solution of Poisson’s equation with free boundary conditions. *J. Chem. Phys.* **2006**, *125*, 074105.
- (74) Genovese, L.; Deutsch, T.; Goedecker, S. Efficient and accurate three-dimensional Poisson solver for surface problems. *J. Chem. Phys.* **2007**, *127*, 054704.
- (75) Perdew, J. P.; Levy, M. Extrema of the density functional for the energy: Excited states from the ground-state theory. *Phys. Rev. B* **1985**, *31*, 6264–6272.
- (76) Xie, B. P.; Zhu, L. F.; Yang, K.; Zhou, B.; Hiraoka, N.; Cai, Y. Q.; Yao, Y.; Wu, C. Q.; Wang, E. L.; Feng, D. L. Inelastic x-ray scattering study of the state-resolved differential cross section of Compton excitations in helium atoms. *Phys. Rev. A* **2010**, *82*, 032501.
- (77) Sekikawa, T.; Okamoto, T.; Haraguchi, E.; Yamashita, M.; Nakajima, T. Two-photon resonant excitation of a doubly excited state in He atoms by high-harmonic pulses. *Opt. Express* **2008**, *16*, 21922–21929.
- (78) Aufleger, L.; Friebel, P.; Rupprecht, P.; Magunia, A.; Ding, T.; Rebholz, M.; Hartmann, M.; Ott, C.; Pfeifer, T. Line-shape broadening of an autoionizing state in helium at high XUV intensity. *New J. Phys.* **2022**, *24*, 013014.
- (79) Schreiber, M.; Silva-Junior, M. R.; Sauer, S. P.; Thiel, W. Benchmarks for electronically excited states: CASPT2, CC2, CCSD, and CC3. *J. Chem. Phys.* **2008**, *128*, 134110.
- (80) Hong, H. K.; Robinson, G. W. The lowest singlet and triplet excited states of pyrazine. *J. Mol. Spectrosc.* **1974**, *52*, 1–20.
- (81) Moule, D. C.; Walsh, A. D. Ultraviolet Spectra and Excited States of Formaldehyde. *Chem. Rev.* **1975**, *75*, 67–84.
- (82) Worth, G. A.; Carley, R. E.; Fielding, H. H. Using photoelectron spectroscopy to unravel the excited-state dynamics of benzene. *Chem. Phys.* **2007**, *338*, 220–227.
- (83) Luis Serrano-Andrés, M. M.; Nebot-Gil, I.; Roos, B. O.; Ischer, M. F. Theoretical Study of the Electronic Spectra of Cyclopentadiene, Pyrrole, and Furan. *J. A. Chem. Soc.* **1993**, *115*, 6184–6197.
- (84) Luis Serrano-Andrés, I. N.-G. R. L., Manuela Merchán; Roos, B. O. Towards an accurate molecular orbital theory for excited states: Ethene, butadiene, and hexatriene. *J. Chem. Phys.* **1993**, *98*, 3151–3162.
- (85) Palmer, M. H.; Jones, N. C.; Hoffmann, S. V.; Aitken, R. A.; Coreno, M.; de Simone, M.; Grazioli, C.; Patterson, I. L. J. The excited states of azulene: A study of the vibrational energy levels for the lower  $\pi\pi^*$ -valence states by configuration interaction and density functional calculations, and theoretical studies of the Rydberg states. *J. Chem. Phys.* **2022**, *157*, 154307.
- (86) Lynam, W. G.; Carroll, P. K.; Costello, J. T.; Evans, D.; O’Sullivan, G. The 1st absorption spectrum of neutral and singly ionized boron. *J. Phys. B: At. Mol. Opt. Phys.* **1992**, *25*, 3963.
- (87) Puchalski, M.; Komasa, J.; Pachucki, K. Testing quantum electrodynamics in the lowest singlet states of the beryllium atom. *Phys. Rev. A* **2013**, *87*, 030502(R).
- (88) Radziemski, L. J.; Engleman, R.; Brault, J. W. Fourier-transform-spectroscopy measurements in the spectra of neutral lithium, I6 and I7 (Li I). *Phys. Rev. A* **1995**, *52*, 4462.
- (89) Behlen, F. M.; McDonald, D. B.; Sethuraman, V.; Rice, S. A. Fluorescence spectroscopy of cold and warm naphthalene molecules: Some new vibrational assignments. *J. Chem. Phys.* **1981**, *75*, 5685–5693.
- (90) Druzhinin, S. I.; Kovalenko, S. A.; Senyushkina, T. A.; Demeter, A.; Zachariasse, K. A. Intramolecular charge transfer with fluorazene and N-phenylpyrrole. *J. Phys. Chem. A* **2010**, *114*, 1621–1632.
- (91) Nagakura, S.; Kojima, M.; Maruyama, Y. Electronic spectra and electronic structures of nitrobenzene and nitromesitylene. *J. Mol. Spectrosc.* **1964**, *13*, 174–192.
- (92) Douglas, A. E.; Greening, F. R. The electronic spectra of HCl and HF. *Can. J. Phys.* **1979**, *57*, 1650–1661.
- (93) Lonardo, G. D.; Douglas, A. E. The Electronic Spectrum of HF. I. The  $B1\Sigma^+ - X1\Sigma^+$  Band System. *Can. J. Phys.* **1973**, *51*, 434–445.
- (94) Burger, S. K.; Yang, W. Linear-scaling quantum calculations using non-orthogonal localized molecular orbitals. *J. Phys.: Condens. Matter* **2008**, *20*, 294209.
- (95) Khaliullin, R. Z.; VandeVondele, J.; Hutter, J. Efficient Linear-Scaling Density Functional Theory for Molecular Systems. *J. Chem. Theory Comp.* **2013**, *9*, 4421–4427.
- (96) Peng, L.; Gu, F. L.; Yang, W. Effective preconditioning for ab initio ground state energy minimization with non-orthogonal localized molecular orbitals. *Phys. Chem. Chem. Phys.* **2013**, *15*, 15518–15527.
- (97) Shi, Y.; Karagunesian, J.; Khaliullin, R. Z. Robust linear-scaling optimization of compact localized orbitals in density functional theory. 2021; <https://arxiv.org/abs/2004.05901>.